

Supporting Information

Strong light-matter interaction and non-linear effects in organic semiconducting CuPc nanotubes: Realization of all-optical diodes and switching applications

Piyali Dey^a, Nabamita Chakraborty^a, Madhupriya Samanta^b, Biswajit Das^c, Kalyan Kumar Chattopadhyay^{a*}

^aThin Film and Nano Science Laboratory, Department of Physics, Jadavpur University, Kolkata 700 032, India

^bSchool of Material Science and Nanotechnology, Jadavpur University, Kolkata 700 032, India

^cDepartment of Basic Science and Humanities, Dr. Sudhir Chandra Sur Institute of Technology and Sports Complex, Kolkata 700074, West Bengal, India

*E-mail address: kalyan_chattopadhyay@yahoo.com (Kalyan K. Chattopadhyay)

S1. Characterization of CuPc dispersion by studying its FT-IR spectra

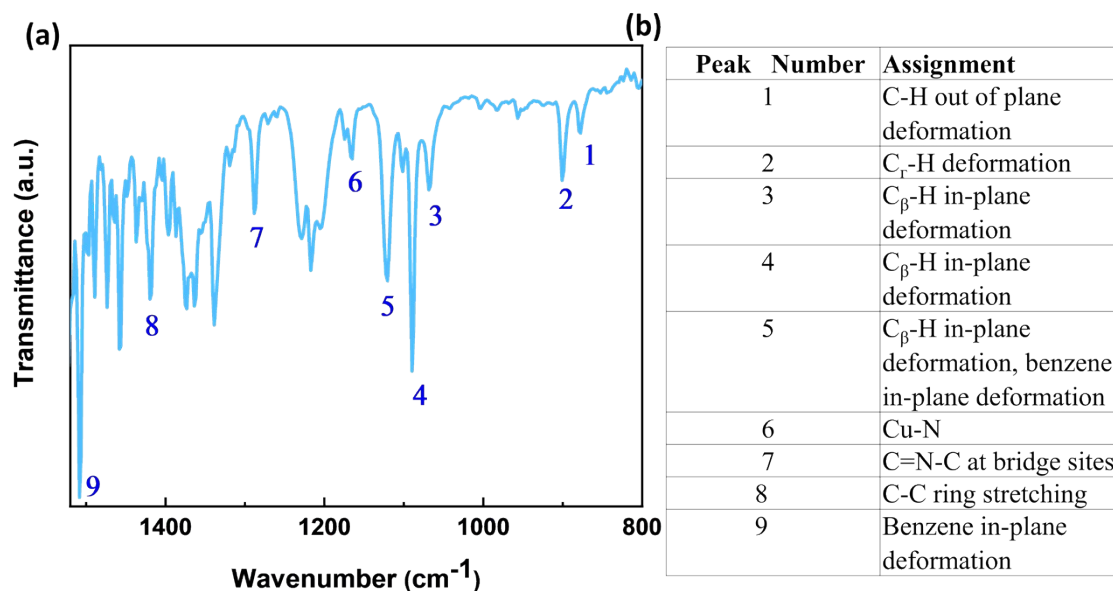


Figure S1. (a) FT-IR spectra of CuPc tube (b) Table showing assignment of the characteristic peaks.

The FTIR analysis was performed by IR Affinity (Spectrum 100, Perkin Elmer) spectrometer to probe the chemical structure of the CuPc nanotubes. The presence of peak at 1166 cm^{-1} confirms the presence of Cu-N bond. Besides, the C=N-C at bridge sites of Phthalocyanine ring is observed at 1287 cm^{-1} . The complete assignment of the IR spectrum peaks in Table S1(b) gives a precise assessment of chemical bonds typically present in CuPc.

S2. Investigation of the light-control-light optical switching response produced in CuPc dispersion

To realize the light-control-light setup, we keep the intensity of the 532 nm laser (signal beam) fixed and vary the intensity of the 671 nm laser (control beam). The signal beam intensity is fixed at 1.273 W/cm^2 below the threshold limit and the intensity of the control

beam is varied. Even though the intensity of the signal beam is below the threshold value the diffraction pattern is obtained and the ring number as a function of the intensity of the control beam is plotted in figure S2. From the graph, it is observed that the ring numbers increase linearly with the control beam intensity. A similar dependence of the ring numbers as a function of control beam intensity is noted for two other signal beam intensities fixed at 2.674 W/cm² and 3.947 W/cm². In the presence of the control beam, the nonlinear polarization at the signal beam frequency induced in the CuPc dispersion depends on the electric field amplitude of the control beam as:¹

$$P^{(\omega_{\text{signal}})} = 6\epsilon_0\chi^{(3)}|E(\omega_{\text{control}})|^2E(\omega_{\text{signal}})$$

where $E(\omega_{\text{control}})$ is the amplitude of the control beam and $E(\omega_{\text{signal}})$ that of the signal beam. This leads to the linear dependence of the signal beam's nonlinear refractive index and nonlinear optical phase shift on the control beam's intensity which explains the behaviour of the graph in S2.

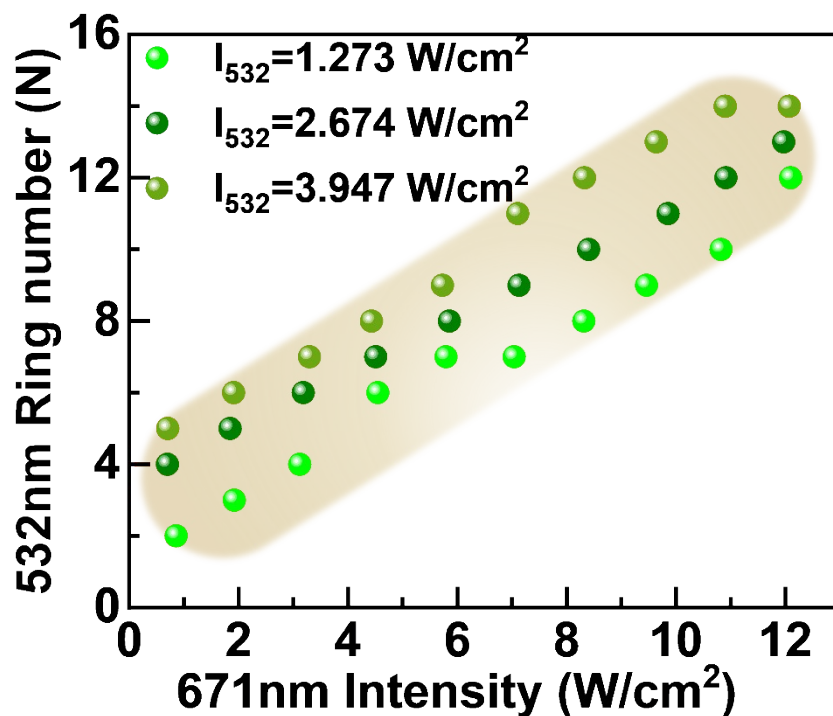


Figure S2. Graph of ring numbers of 532 nm laser for three fixed intensities at 1.273 W/cm², 2.674 W/cm² and 3.947 W/cm² vs intensity of 671 nm laser.

S3. Estimation of single layer nonlinear susceptibility of CuPc Nanotube

To compare with the nonlinear optical susceptibility of different nanomaterials, the $\chi_{\text{singlelayer}}^{(3)}$ of CuPc nanotubes have been estimated. Unlike 2D layered materials, the CuPc nanotube does not have well defined single layers separated by van der Waals force. So we have considered the calculation of electron density layer in the a-b plane of the unit cell of CuPc.² It has a monoclinic symmetry with 2 molecules per unit cell.³

For a fixed concentration of CuPc dispersion (0.125 mg/ml), the number of unit cells (M) in the cuvette of volume 3.5 ml are estimated. Then the number of cells that cover an

effective layer is found ($m = \frac{\text{area of lateral surface of cuvette}}{\text{unit cell area in a - b plane}}$). This gives the effective

number of charge density layers that the laser beam travels through as $N_{\text{eff}} = \frac{M}{m} = 531$ layers.

The resultant $\chi_{\text{singlelayer}}^{(3)}$ is calculated as:

$$\chi_{\text{total}}^{(3)} = N_{\text{eff}}^2 \chi_{\text{singlelayer}}^{(3)}$$

The N_{eff} and $\chi_{\text{singlelayer}}^{(3)}$ is calculated for 3 wavelength of light, 3 different concentration, 3 different cuvette length and listed in the following table.

Table S1. Nonlinear susceptibility $\chi_{\text{singlelayer}}^{(3)}$ of CuPc nanotube

Wavelength (nm)	Length (mm)	Concentration (mg/ml)	dN/dI (cm ² /W)	n ₂ (×10 ⁻⁵) (cm ² /W)	χ ⁽³⁾ _{total} (×10 ⁻³) (esu)	N _{eff}	χ ⁽³⁾ _{singlelayer} (×10 ⁻⁹) (esu)
671	10	0.125	1.149	2.62	1.44	531	5.12
532	10	0.125	1.463	2.65	1.45	531	5.14
405	10	0.125	2.662	3.66	2.01	531	7.13

671	10	0.0625	0.860	1.96	1.08	266	1.53*10
671	10	0.03125	0.521	1.19	0.65	133	3.69*10
671	5	0.125	0.923	4.01	2.20	258	3.31*10
671	1	0.125	0.366	8.37	4.59	53	1.63*10 ³

S4. Estimation of Band Gap from Diffuse Reflectance Spectroscopy

We have calculated the bandgap energy of CuPc nanotubes by measuring the diffuse reflectance spectroscopy from the UV-Vis Spectrophotometer. The Kubelka Munk theory is applied to calculate the Kubelka Munk function :⁴

$$F(R_{\infty}) = \frac{(1 - R_{\infty})^2}{2R_{\infty}} = \frac{k}{s}$$

Where R_{∞} is the experimentally found reflectance of the sample and k , s are the absorption and the scattering coefficient respectively. The bandgap is calculated from the Tauc plot of the reflectance data by plotting $(F(R_{\infty})h\nu)^{1/\gamma}$ as a function of $h\nu$ of the incident light. Since CuPc has a direct bandgap so $\gamma = 1/2$. From the expression $(F(R_{\infty})h\nu)^2 = B(h\nu - E_g)$, the bandgap is determined by extrapolating the linear region of the graph where it intersects the x axis. This way the bandgap is found as 1.7 eV for CuPc.

S5. Correlation of $\chi^{(3)}$ _{singlelayer} with carrier mobility for nanomaterials exhibiting SSPM

We verify the proposed electronic origin of SSPM by investigating the correlation of nonlinear susceptibility and the charge carrier mobility for 2D layered materials like graphene^{5, 6}, black phosphorus^{7, 8}, MoS₂^{9, 10}, MoTe₂¹¹, MoSe₂¹², 3D TaAs² and CuPc. Except CuPc all other values are obtained from reference. CuPc is a p type material so it can be said that the holes predominantly participate in the ring formation process. The hole mobility of

CuPc is $171.8 \text{ cm}^2\text{V}^{-1}\text{s}^{-1}$ ¹³ and the $\chi_{\text{singlelayer}}^{(3)}$ value of 5.14×10^{-9} e.s.u. obtained from our work is plotted which follows the same trend as that of other nanomaterials.

The positive correlation between carrier mobility and the susceptibility values (Figure S3) reinforce the laser induced electron or hole coherence mechanism as the origin of SSPM.

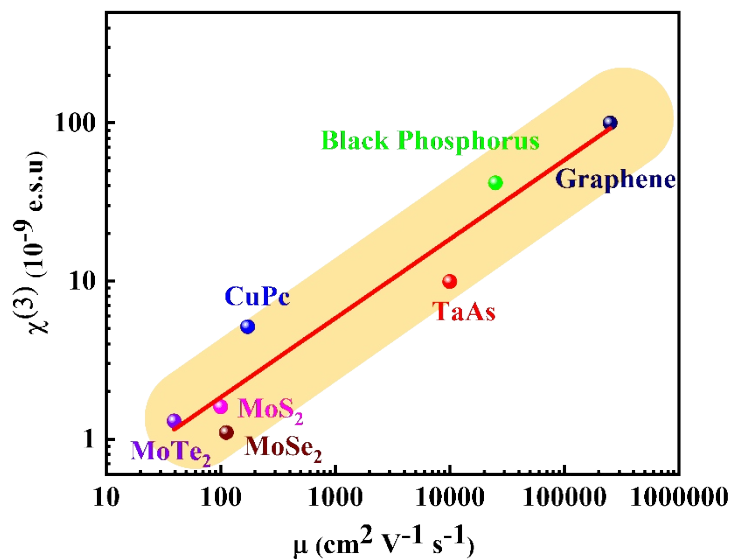


Figure S3. Linear correlation between charge carrier mobility and $\chi_{\text{singlelayer}}^{(3)}$ obtained from SSPM for different nanomaterials (adapted from reference 5-13), and CuPc.

S6. Stability and repeatability data of photonic devices

The application of CuPc dispersion in constructing all-optical diodes and logic gates has been presented in our work. For practical application purpose, long-term stability and repeatability are crucial. Hence, we performed the experiment with the same dispersion after 17 months. It is found from the data that the forward and reverse slope remains almost same for the green and red laser. We also performed the logic gates application on the same dispersion after the same time-period and found the system to properly exhibit the logical OR operation. Thus, we can conclude that the system remains stable and repeatability is maintained.

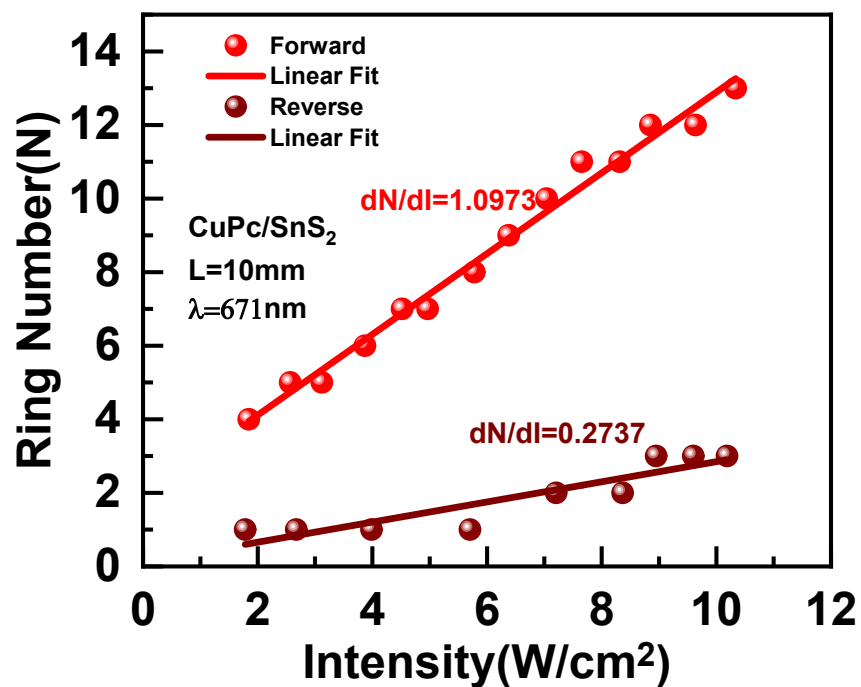


Figure S4. Plot of ring number vs intensity in forward and reverse optical path for 671 nm laser in repeatability test work

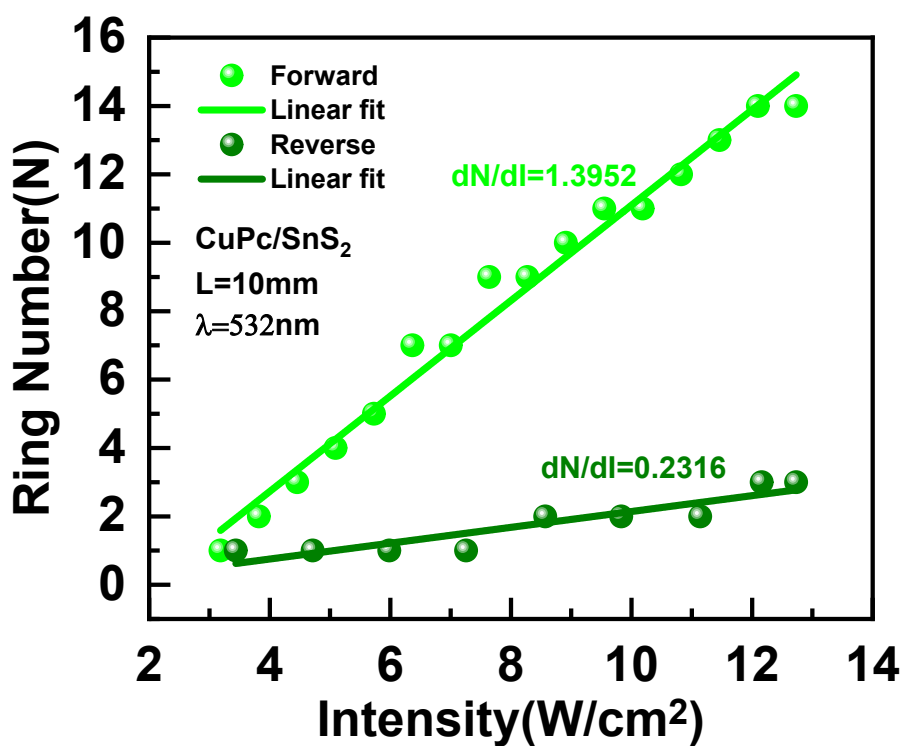


Figure S5.: Plot of ring number vs intensity in forward and reverse optical path for 532 nm laser in repeatability test work

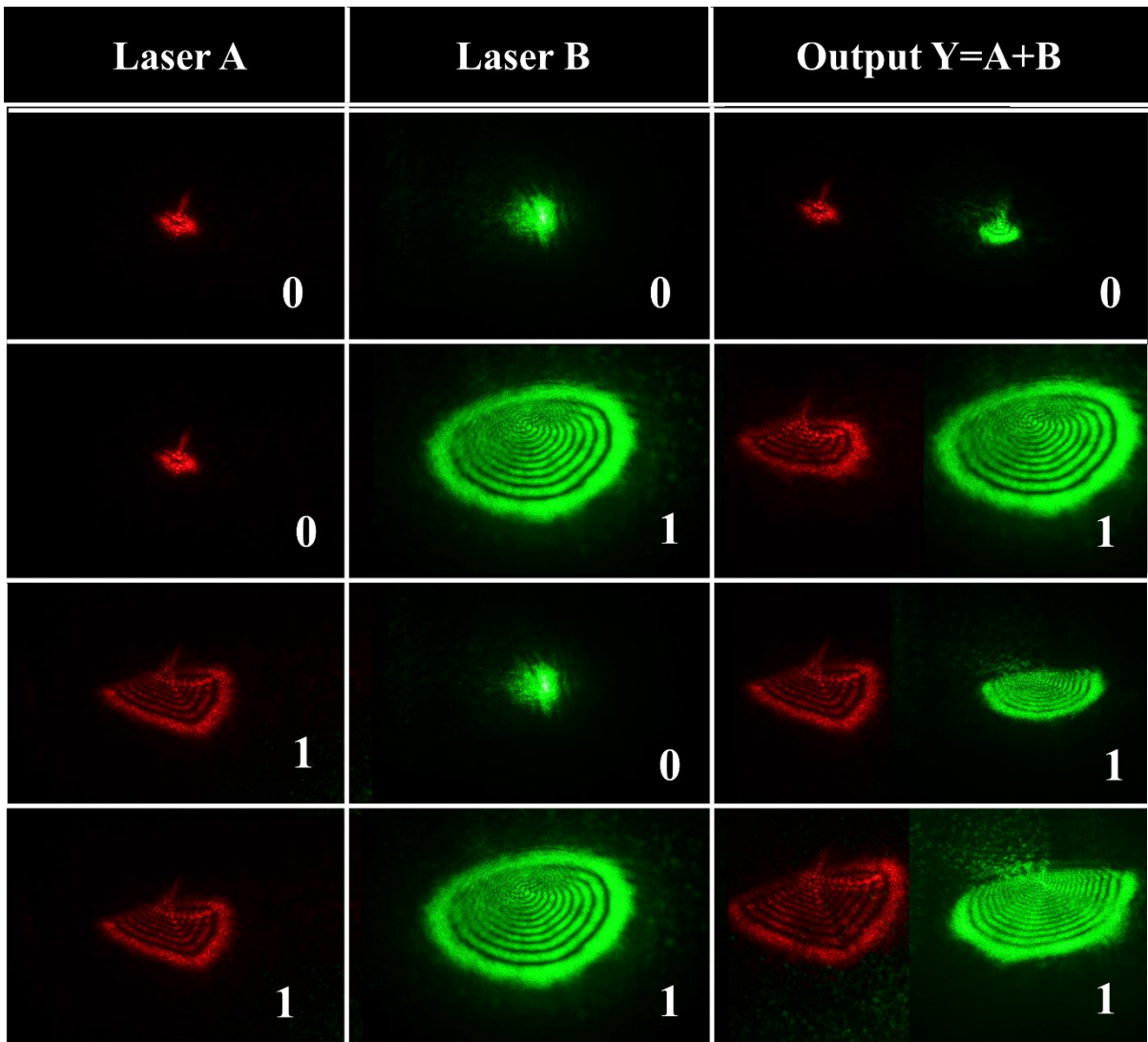


Figure S6.: Images of optical logic OR Gate by cross coupling beams of 671nm and 532 nm as obtained in repeatability test work

S7. Comparison of reported nanomaterial's Kerr coefficient with CuPc

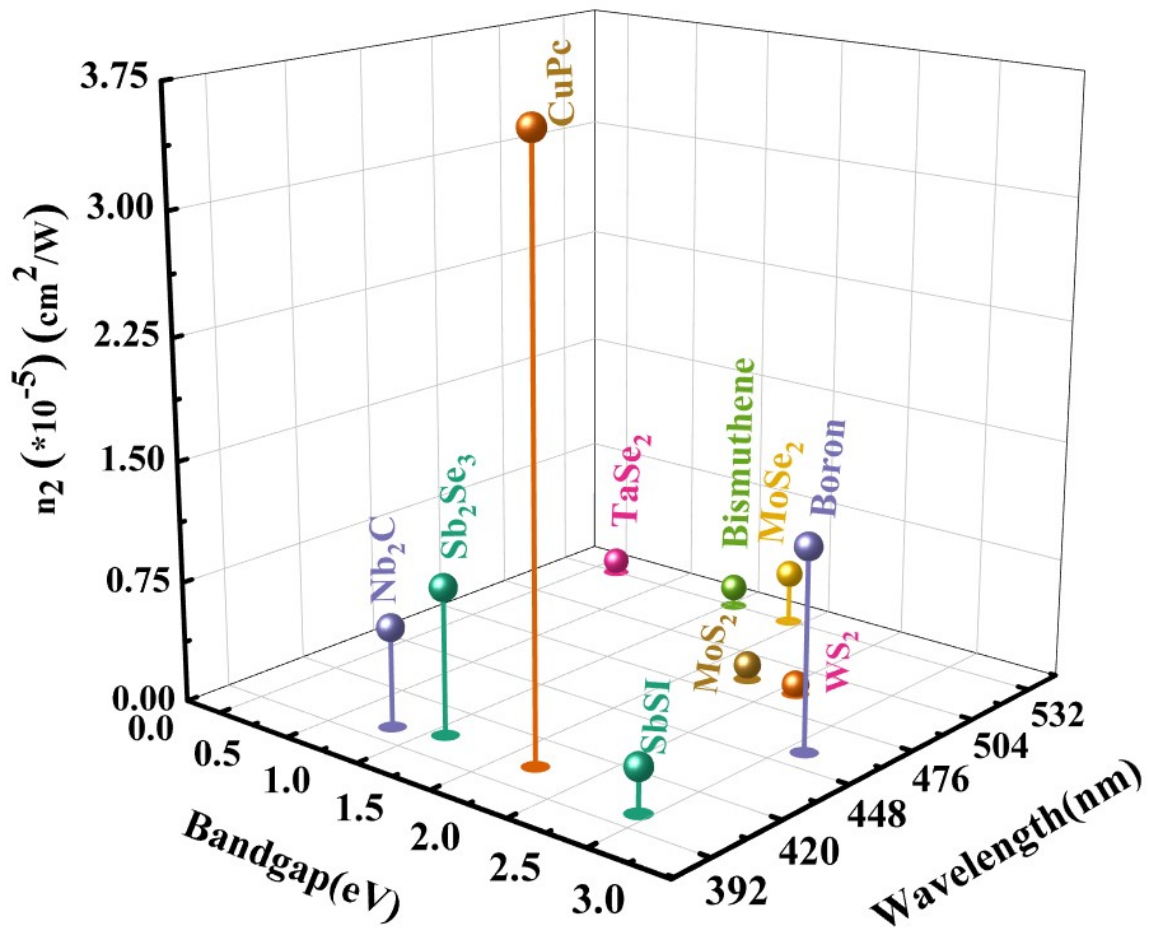


Figure S7.: Graphical representation of comparison of reported nanomaterial's Kerr coefficient with CuPc

References:

1. R. W. Boyd, in *Nonlinear Optics (Third Edition)*, ed. R. W. Boyd, Academic Press, Burlington, 2008, DOI: <https://doi.org/10.1016/B978-0-12-369470-6.00004-6>, pp. 207-252.
2. Y. Huang, H. Zhao, Z. Li, L. Hu, Y. Wu, F. Sun, S. Meng and J. Zhao, *Advanced Materials*, 2023, **35**, 2208362.
3. L. Lozzi, S. Santucci, S. La Rosa, B. Delley and S. Picozzi, *The Journal of Chemical Physics*, 2004, **121**, 1883-1889.
4. P. Makuła, M. Pacia and W. Macyk, *The Journal of Physical Chemistry Letters*, 2018, **9**, 6814-6817.
5. R. Wu, Y. Zhang, S. Yan, F. Bian, W. Wang, X. Bai, X. Lu, J. Zhao and E. Wang, *Nano Letters*, 2011, **11**, 5159-5164.
6. M. Orlita, C. Faugeras, P. Plochocka, P. Neugebauer, G. Martinez, D. K. Maude, A. L. Barra, M. Sprinkle, C. Berger, W. A. de Heer and M. Potemski, *Physical Review Letters*, 2008, **101**, 267601.
7. J. Zhang, X. Yu, W. Han, B. Lv, X. Li, S. Xiao, Y. Gao and J. He, *Opt. Lett.*, 2016, **41**, 1704-1707.
8. G. Long, D. Maryenko, J. Shen, S. Xu, J. Hou, Z. Wu, W. K. Wong, T. Han, J. Lin, Y. Cai, R. Lortz and N. Wang, *Nano Letters*, 2016, **16**, 7768-7773.
9. Y. Wu, Q. Wu, F. Sun, C. Cheng, S. Meng and J. Zhao, *Proceedings of the National Academy of Sciences*, 2015, **112**, 11800-11805.
10. S.-L. Li, K. Tsukagoshi, E. Orgiu and P. Samorì, *Chem Soc Rev*, 2016, **45**, 118-151.
11. L. Hu, F. Sun, H. Zhao and J. Zhao, *Opt. Lett.*, 2019, **44**, 5214-5217.
12. W. Wang, Y. Wu, Q. Wu, J. Hua and J. Zhao, *Scientific Reports*, 2016, **6**, 22072.
13. S. Pengmanayol, T. Osotchan, M. Suewattana, N. Ingadapa and J. Girdpun, *Chinese Physics Letters*, 2011, **28**, 086103.